NEUROSCIENCE of Consciousness

Neuroscience of Consciousness, 2022, **2022(1)**, 1–15

DOI: https://doi.org/10.1093/nc/niac004

Research Article

Special Issue: Consciousness science and its theories

Capacity for consciousness under ketamine anaesthesia is selectively associated with activity in posteromedial cortex in rats

A. Arena[1,*,†], B. E. Juel[1,2,‡], R. Comolatti[3], S. Thon[1], and J. F. Storm[1]

[1]Brain Signalling Group, Department of Molecular Medicine, University of Oslo, Sognsvannsveien 9, Oslo 0372, Norway; [2]Center for Sleep and Consciousness, University of Wisconsin, 6001 Research Park Blvd, Madison, WI 53719, USA;[3]Department of Biomedical and Clinical Sciences "L. Sacco", University of Milan, Via Giovanni Battista Grassi 74, Milano 20157, Italy

[†]A. Arena, http://orcid.org/0000-0002-3192-2265

[‡]B. E. Juel, http://orcid.org/0000-0003-0550-581X

*Correspondence address. Brain Signalling Group, Department of Molecular Medicine, University of Oslo, Sognsvannsveien 9, Oslo 0372, Norway. Tel: (+47) 22850132; E-mail: alessandro.arena@medisin.uio.no

Abstract

It remains unclear how specific cortical regions contribute to the brain's overall capacity for consciousness. Clarifying this could help distinguish between theories of consciousness. Here, we investigate the association between markers of regionally specific (de)activation and the brain's overall capacity for consciousness. We recorded electroencephalographic responses to cortical electrical stimulation in six rats and computed Perturbational Complexity Index state-transition (PCI^{ST}), which has been extensively validated as an index of the capacity for consciousness in humans. We also estimated the balance between activation and inhibition of specific cortical areas with the ratio between high and low frequency power from spontaneous electroencephalographic activity at each electrode. We repeated these measurements during wakefulness, and during two levels of ketamine anaesthesia: with the minimal dose needed to induce behavioural unresponsiveness and twice this dose. We found that PCI^{ST} was only slightly reduced from wakefulness to light ketamine anaesthesia, but dropped significantly with deeper anaesthesia. The high-dose effect was selectively associated with reduced high frequency/low frequency ratio in the posteromedial cortex, which strongly correlated with PCI^{ST}. Conversely, behavioural unresponsiveness induced by light ketamine anaesthesia was associated with similar spectral changes in frontal, but not posterior cortical regions. Thus, activity in the posteromedial cortex correlates with the capacity for consciousness, as assessed by PCI^{ST}, during different depths of ketamine anaesthesia, in rats, independently of behaviour. These results are discussed in relation to different theories of consciousness.

Keywords: consciousness; ketamine anesthesia; EEG markers of consciousness; perturbational complexity index

Highlights

- We dissociate responsiveness from consciousness using a two-level ketamine protocol in rats.
- We correlate activity in cortical regions with PCI^{ST}, an indicator of capacity for consciousness.
- Cortical deactivation in the back, but not the front, was associated with a significant drop in PCI^{ST}.

Introduction

It is widely recognized that only a limited fraction of our brain activity is directly involved in specifying our conscious experience (Koch *et al.* 2016). Ideally, a theory of consciousness should be able to precisely explain why only certain parts of the brain and types of activity contribute to any particular experience. This reflects two main aspects of consciousness science: understanding which brain structures and activities are required for having a capacity for consciousness, and which are required for particular contents

Received: 15 January 2021; **Revised:** 9 December 2021; **Accepted:** 24 January 2022

© The Author(s) 2022. Published by Oxford University Press.

This is an Open Access article distributed under the terms of the Creative Commons Attribution License (https://creativecommons.org/licenses/by/4.0/), which permits unrestricted reuse, distribution, and reproduction in any medium, provided the original work is properly cited.

of conscious experience. The former can be identified by studying how properties of brain activity change between brain states where the level of consciousness is thought to change, such as comparing wakefulness with deep, general anaesthesia or dreamless sleep (e.g. Casali et al. 2013). The latter can be identified by contrasting brain activity between conditions where particular stimuli are perceived or not, without otherwise altering the level of consciousness (e.g. van Vugt et al. 2018).

Recently, the roles played by the frontal vs. posterior parts of the neocortex in the consciousness of healthy humans have been discussed (Boly et al. 2017; Odegaard et al. 2017). In this 'front vs. back debate', some have argued that the 'evidence for a direct, content-specific involvement of the "front" of the cortex, including most prefrontal regions, is missing or unclear' (Boly et al. 2017), while others argued that 'the literature highlights prefrontal cortex's essential role in enabling the subjective experience in perception' (Odegaard et al. 2017). Although this debate largely concerned empirical data, and the issue remains unresolved, the debate illustrates that different theories of consciousness entail different hypotheses about which brain regions contribute directly to experience and which provide necessary background conditions for consciousness. Hence, evidence showing regional differences in contribution to the capacity for, or contents of, consciousness may provide specific empirical support for some theories over others.

Some authors have suggested that frontal parts of the cortex are crucial for consciousness (Del Cul et al. 2009) or have decoded perceptual contents from frontal regions (Levinson et al. 2021). Thus, the prefrontal cortex was found to be causally involved in determining the contents of experience (Weilnhammer et al. 2021), and frontal neuronal activity correlated with visual perception (even during no-report paradigms; Kapoor et al. 2020). However, others have pointed to evidence that the apparent frontal involvement in consciousness may be confounded with task-related processes such as working memory, attention, or preparation for motor response (Koch et al. 2016; Boly et al. 2017). While this does not imply that frontal cortical regions are not necessary for, or causally involved in, specifying human experiences, it does remind us that brain functions associated with normal behavioural responsiveness can be confounded with those directly involved in specifying conscious experiences (Sanders et al. 2012).

The ability to respond coherently to external stimuli is used as the main criterion for determining whether non-communicating patients and non-human animals are conscious (Chernik et al. 1990; Giacino et al. 2004; Gao and Calderon 2020). However, this approach is based on the assumption that unresponsive states are always unconscious, which is at odds with evidence that vivid experiences can occur in unresponsive states. For instance, dreams can occur in all stages of sleep (Nielsen 2000; Solms 2000; Siclari et al. 2018) and during general anaesthesia (Noreika et al. 2011). Furthermore, patients can be conscious but unresponsive for decades after brain damage(Vanhaudenhuyse et al. 2018), or they can be painfully aware during general anaesthesia for surgery, while assumed to be unconscious (Ghoneim et al. 2009). Conversely, quite complex behaviours can be preserved during conditions that are typically assumed to be unconscious, e.g. sleepwalking, sleep talking (Castelnovo et al. 2018; Valomon et al. 2021), and presumed unconscious behaviours during certain epileptic seizures, and in unresponsive wakefulness syndrome (Blumenfeld 2005; Laureys et al. 2010). Thus, it is essential to distinguish brain regions necessary for consciousness from those that are necessary for behavioural responsiveness.

Recently, several measures aiming to objectively assess global states of consciousness independently of motor or sensory functions have been developed (see for example Luppi et al. 2021), with a notable convergence in evaluating the complexity of brain activity as indication of the capacity for consciousness (Sarasso et al. 2021). In particular, the perturbational complexity index [PCI; (Casali et al. 2013)], and the more general measure PCI^{ST} ['PCI-state transition'; (Comolatti et al. 2019)], have been shown to reliably and consistently assess the capacity for consciousness in humans in accordance with the subjects' immediate or delayed reports of experience (Sarasso et al. 2015; Casarotto et al. 2016; Rosanova et al. 2018). Recently, PCI^{ST} has also been shown to work consistently in rodents undergoing propofol, sevoflurane, and ketamine anaesthesia (Arena et al. 2021). PCI and PCI^{ST} quantify the spatiotemporal complexity of repeatable, global, cortical, electrophysiological responses to a local, direct cortical stimulation, thus estimating how much the resulting deterministic neuronal activations are both integrated and differentiated across cortical areas and time. PCI is inspired by the general idea that the joint presence of integration and differentiation is required for a system to be conscious, which is a central part of the Integrated Information Theory (IIT; Tononi 2004; Massimini et al. 2009). Later on, PCI has also been considered to be compatible with the Global Neuronal Workspace (GNW) Theory, as the measure is sensitive to global and sustained patterns of cortical interaction (Baars 2005; Dehaene et al. 2011; Mashour et al. 2020). More importantly, PCI may be considered an index of capacity for consciousness even in cases where we do not know the ground truth (Casarotto et al. 2016; Comanducci et al. 2020). Therefore, for the remainder of this paper, we interpret a significant drop in PCI from what is observed in wakefulness as indicative of a relative reduction in capacity for consciousness.

While PCI is an index of the capacity for consciousness based on evoked cortical dynamics, measures that quantify spectral properties of spontaneous cortical activity have also for long been used successfully to study brain states (Loomis et al. 1937; Fernandez et al. 2017; Siclari et al. 2017; Colombo et al. 2019; Lendner et al. 2020). In particular, during deep stages of sleep and general anaesthesia, both electroencephalography (EEG) and local field potentials are characterized by high amplitude, low frequency (LF, ≤ 4 Hz) oscillations or slow-waves (Massimini et al. 2004; Vyazovskiy et al. 2009; Brown et al. 2010). This slow-wave activity reflects a bistable network dynamic, where neurons synchronously alternate between an up-state, with depolarized membrane potential and firing, and a down-state with neuronal hyperpolarization and silence (Steriade et al. 1993, 2001; Volgushev et al. 2006; Vyazovskiy et al. 2009), possibly due to increased inhibition, adaptation, and synaptic fatigue (Steriade et al. 2001; Compte et al. 2003; Esser et al. 2007; Funk et al. 2017). Conversely, during wakefulness, the EEG is mainly characterized by low amplitude, high frequency (HF, ≥ 20 Hz) oscillations, which reflect tonic neuronal depolarization and firing (Steriade et al. 1996, 2001; Mukovski et al. 2007; Vyazovskiy et al. 2009). This has inspired several measures for quantifying the cortical state of activation based on the relation between high (HF) and low (LF) frequency EEG power (Mukovski et al. 2007; Fernandez et al. 2017; Gao et al. 2017; Siclari et al. 2017; Colombo et al. 2019; Lendner et al. 2020). Thus, the HF/LF (power) ratio tends to drop when there is more inhibition and deactivation, whereas a higher HF/LF ratio suggests neuronal activation (Mukovski et al. 2007; Gao et al. 2017; Lombardi et al. 2017; Poulet and Crochet 2018). Coherently, the spectral relation between HF and LF powers has been associated with

the excitation/inhibition balance (Gao *et al.* 2017) and the ratio between LF and HF powers was found to correlate with motor activity in mice (Fernandez *et al.* 2017). Thus, local changes in HF/LF ratio may indicate changes in cortical activation (Poulet and Crochet 2018).

While measures of consciousness typically evaluate global brain dynamics, specific and localized changes in the HF/LF ratio may occur within the same brain state and might affect behaviour or conscious experience. For example, local cortical sleep, which can affect task performance in rats, involves localized slow waves and neuronal silence in an otherwise awake brain state, dominated by low amplitude and fast oscillations, with underlying tonic neuronal firing (Vyazovskiy *et al.* 2011). Furthermore, posterior increases in HF/LF ratio during deep stages of sleep successfully predicted whether or not humans reported dreaming and were explained by a simultaneous local reduction of 1–4 Hz activity and enhanced 20–50 Hz activity (Siclari *et al.* 2017). Thus, HF/LF can vary regionally within global states, but it is not known whether local reductions in HF/LF are associated with reduced consciousness levels. More generally, it is still unknown whether any particular localized spectral properties are related to the brain's global capacity to sustain consciousness.

In this study, we aimed at investigating this relation, asking whether specific regional changes of cortical activation, assessed by the HF/LF ratio, are associated with changes in capacity for consciousness, assessed by PCI^{ST}, irrespectively on the specific content of experience. We also aimed to dissociate levels of behavioural (un)responsiveness (assessed by responses to pain stimuli) from the capacity for consciousness by comparing wakefulness with two distinct levels of ketamine anaesthesia. Indeed, it has been shown that the unresponsive state induced by ketamine can subtend vivid conscious experiences, with wakefulness-like, high PCI (Sarasso *et al.* 2015; Arena *et al.* 2021). While it was also previously reported that when ketamine plasma level is particularly high, such as soon after bolus injection (Akeju *et al.* 2016), the EEG alternates between low and highly complex activity patterns (Li and Mashour 2019). In this condition, slow-wave oscillations also occur, interrupting an enhanced HF activation, resulting in the gamma-burst activity pattern (Akeju *et al.* 2016; Li and Mashour 2019), and suggesting transient moments of unconsciousness at high ketamine doses. Here, we carefully control ketamine dosage by adopting intravenous infusion at two different constant rates and infer conscious experience relying on PCI^{ST} level, in comparison with wakefulness condition. Then, we investigate whether regional HF/LF ratio reliably covaries with changes in PCI^{ST}, within and across conditions. The results may be used to validate predictions and explanations from theories of consciousness by constraining which cortical regions mainly underlie consciousness as opposed to behavioural responsiveness.

Materials and methods

Animal model and experimental data

Six adult, male, Sprague–Dawley rats ($n = 6$; body weight ~370 g) were used in this study. All the experiments and animal care procedures were conducted at the University of Oslo and were approved by the Norwegian Authority, Mattilsynet (FOTS: 11812) in agreement with the Norwegian law of animal handling. Efforts were made to avoid or minimize animals' pain and distress. Rats were caged in enriched environments, with *ad libitum* access to food and water and were exposed to a 12:12 hour light–dark cycle at 23°C constant room temperature.

In addition to new data, we also included a new analysis of data from a set of previously published experiments (Arena, Thon and Storm, 2019; Arena *et al.* 2021) with a new analysis. Specifically, we reanalysed data from a subset of six rats, from which we recorded epidural EEG continuously and in response to electrical stimulation of the secondary motor cortex during wakefulness and light ketamine anaesthesia (Arena *et al.* 2021). These data will be compared to those from a new set of recordings/stimulations that were performed on the same six rats during a subsequent period of ketamine anaesthesia with increased dosage.

Experimental procedure

Epidural EEG was recorded by a grid of 16 screw electrodes (stainless steel, 1.2 mm calibre), which were chronically implanted through the skull, in contact with the dura. The recording electrodes were organized symmetrically with respect to the sagittal suture and spanned most of the cortical surface of both hemispheres (Supplementary Fig. S1). The bilateral frontal cortex was covered by six electrodes, named $M2_R$, $M2_C$ and M2/M1 that medially overlaid the rostral and caudal part of the secondary motor cortex and part of the primary motor cortex, respectively. Other six electrodes covered left and right parieto-occipital associative cortices: PA electrodes covered lateral parietal cortex, RS/PA medially covered retrosplenial and parietal cortex, while RS/V2 electrodes covered the posteromedial cortex, over the caudal part of retrosplenial cortex and medial part of secondary visual cortex. The last four electrodes, bilateral S1 and V1, overlaid the primary somatosensory cortex and the primary visual cortex respectively. Event-related potentials (ERPs) were recorded in response to electrical stimulation of the right secondary motor cortex by a bipolar tungsten electrode (see Supplementary Fig. S1 for detailed electrode locations with respect to bregma; Paxinos and Watson 2007). The standard surgical procedure under a regime of controlled general anaesthesia/analgesia was adopted for implantation of chronic electrodes, and after 3 days of recovery, rats were habituated to head and body restriction in at least 3 subsequent days, as previously described (Arena *et al.* 2021). The electrophysiological recording/stimulation began only when rats did not show any sign of distress and were calm within the recording setup, with the head connected to a fixed head-bar by two chronically implanted clamps and with the body inserted in a transparent acrylic tube, with a natural posture. The tail was left outside the tube to test reflex motor responses to pain stimulation.

The six rats were subjected to electrophysiological recording/stimulation sessions during wakefulness and subsequent ketamine anaesthesia. Ketamine (Vetoquinol, Ittigen, Switzerland) was infused at a constant rate via a 26 GA catheter in the tail vein. Subcutaneous injection of glycopyrrolate 0.01 mg/kg was also performed to reduce the increased salivation. Since rats keep eyes open during general anaesthesia, eye ointment was applied to maintain eyes humid and body temperature was kept at 36.5–37.5°C by a heating pad, as previously described in detail. During the recording session, the stimulating electrode was connected to an isolated current stimulator (Isolator HG203, High Medical, London, UK) triggered by a voltage pulse generator (2100, A-M System, Washington DC, USA), while the epidural EEG electrodes were connected to a 16-channel unipolar amplifier referenced to ground (RHD2132, Intan Technologies, Los Angeles, CA, USA), and controlled by Open Ephys system (Siegle *et al.* 2017), which acquired and digitized the electrophysiological signal at 10 or 30 kHz, 16-bit resolution.

The EEG activity was continuously recorded from all 16 channels, in a dark environment, in which all rats received

~100 electrical monophasic current pulses of 50 μA, 1 ms, delivered at 0.1 Hz, at first during wakefulness (W), and during subsequent ketamine anaesthesia. The anaesthesia was induced by an intravenous (iv) bolus injection of ketamine 30 mg/kg and then maintained at the initial constant rate of ketamine 1.75 mg/kg/min iv, by a syringe pump. After 10 min from induction, the tail was pinched three times by forceps to check the presence of behavioural reaction to pain stimulation. The behavioural response typically consisted of a lateral and wide movement of the tail and/or in the alteration of the respiratory rhythm, with the occurrence of a deeper breath, accompanied by a sudden chest movement. The infusion rate was stepwise increased by adding 4% of the initial dosage until the behavioural response was absent (3 min between each increment). The resulting minimal dosage of ketamine that abolished behavioural reaction to pain stimulation was 1.78 ± 0.02 mg/kg/min, iv (mean ± SEM across rats; 1.8 mg/kg/min for simplicity) and defined the condition 'ketamine 1' or K1. In order to evaluate possible dose dependencies, the same recording/stimulation was also repeated afterwards, during deeper ketamine anaesthesia ('ketamine 2' or K2), at the constant rate of 3.5 mg/kg/min iv, which corresponded to two times the initial constant rate.

Analysis of electrophysiological signal

The acquired electrophysiological data were analysed in MATLAB2016a (Math Works, Natick, Massachusetts, USA) and Origin 9.1 (OriginLab, Northampton, Massachusetts, USA) and preprocessed as described before (Arena *et al.* 2021). Raw epidural EEG was bandpass filtered (0.5–80 Hz, Butterworth, third order), downsampled to 500 Hz and ERP epochs of 10 s were extracted for each channel, centred at the stimulus onset (from –5 to 5 s). All epochs were offset corrected by subtracting the average voltage of their respective baseline (from –1 to 0 s), and trials with high voltage artefacts in their baseline were removed. The first 90 trials of preprocessed signals were used for analysis, maintaining the same temporal sequence across animals and conditions. ERPs were not normalized and the electrical noise was similar along with the whole duration of recordings.

The cortical excitation in response to electrical stimulation was quantified by the root mean squared (rms) amplitude of the first 50 ms of the mean ERP for all electrodes, and then averaged across electrodes. Spectral powers and phases of ERPs were obtained from Morlet wavelet convolution (three cycles wavelets, linearly spanning from 1 to 80 Hz, with 1 Hz resolution), which was performed for each trial and channel. The spectral powers were normalized over the mean power of the baseline (–500 to –200 ms) across trials, for each respective frequency and channel. The mean relative powers across trials were then dB converted and bootstrap statistic (500 permutations; positive and negative thresholds based on the obtained distribution of the maximum and minimum dB values in the baseline window, $\alpha = 0.05$) was applied for each frequency and channel to conserve only the significant dB variations from respective baseline. The resulting relative spectral power was averaged across trials in the HF range (20–80 Hz) to estimate the temporal dynamic of the neuronal activation underlying the EEG signal (Mukovski *et al.* 2007; Pigorini *et al.* 2015; Rosanova *et al.* 2018; Arena *et al.* 2021). Late increments of HF power (> 0 dB) were detected in a time window from 80 to 800 ms (Arena *et al.* 2021). The inter-trial phase clustering [ITPC; (Cohen 2014)] was computed for each frequency and channel and bootstrap statistic (500 permutations; threshold based on the obtained distribution of the maximum ITPC values in the baseline window, $\alpha = 0.01$) was used to conserve only the ITPC increments that differed significantly from the respective baseline (from –500 to –200 ms). The time point of the last significant ITPC value within 800 ms after stimulation and in a broad frequency range (5-80 Hz) was detected for each channel and considered to be the duration of the phase-locked EEG response, which quantified the temporal extension of the deterministic effect of the electrical stimulation [ITPC drop time; (David *et al.* 2006; Pigorini *et al.* 2015; Rosanova *et al.* 2018; Arena *et al.* 2021)]. PCI^{ST} was used to estimate the capacity for consciousness (Comolatti *et al.* 2019; Arena *et al.* 2021) and was assessed in the full ERP window, from 0 to 600 ms, and across time, in short, moving windows of 100 ms, with 50 ms of overlap. PCI^{ST} was computed using the available code at [github.com/renzocom/PCIst] with the same parameters previously described (Comolatti *et al.* 2019; Arena *et al.* 2021). The functional connectivity across cortical areas in response to stimulation was also used to estimate the level of integration and differentiation of the cortical network, as previously described in detail (Arena *et al.* 2021). The inter-site phase clustering (ISPC) was assessed as the consistency across trials of the phase difference across channels for all time-frequency points (Cohen 2014; Arena *et al.* 2021). ISPC was calculated for each channel pair, the respective mean ISPC of the baseline (from –500 to –200 ms) was subtracted and bootstrap statistic (500 permutations; positive and negative thresholds based on the obtained distribution of the maximum and minimum ISPC values in the baseline window, $\alpha = 0.05$) was adopted to conserve only the significant variations from baseline. The ISPC values that could be determined by volume conduction (clustering around 0 or pi) were set to 0 and the remaining ISPC values were averaged in the frequency range 5–14 Hz and between 180 and 400 ms. The proportion of the number of mean positive ISPC values for each channel was defined as the connectivity degree of the electrode (Cohen 2014; Arena *et al.* 2021).

The spontaneous cortical activity associated with the different experimental conditions was quantified from 90 epochs of 5 s of epidural EEG signal that preceded the electrical stimulation (from –5 to 0 s). A Morlet wavelet convolution (6 cycles, 80 wavelets, linearly spanning from 1 to 80 Hz) was performed on each epoch for all channels. Spectral powers were extracted and averaged across samples, trials and channels, obtaining a global estimation of the power of each frequency for each animal and condition. The resulting periodogram was linearly fitted in Log-Log coordinates, in the frequency range 20–40 Hz. The slope of the obtained linear function was the spectral exponent of the 1/f function and was used to quantify the distribution of frequency powers in the spontaneous EEG activity (Gao *et al.* 2017; Colombo *et al.* 2019; Lendner *et al.* 2020; Arena *et al.* 2021). Instantaneous powers were normalized by 1 and converted in dB, and also averaged in high and low frequency ranges (HF 20–80 Hz, LF 1–4 Hz, respectively), across and for each single channel, before dB conversion. The ratio between HF power and LF power (HF/LF ratio) was also computed to estimate the level of activation for the cortical area underlying each channel (Fernandez *et al.* 2017; Poulet and Crochet 2018) and its contribution to cortical complexity and capacity for consciousness (Siclari *et al.* 2017).

Statistics

All results are expressed as mean ± SEM and error bars and shades represent SEM in the figures. Shades in linear regressions represent the 95% confidence band. The topographical plots in the

figures report the Laplace interpolation of a variable over the dorsal surface of a skull, anchored to the true electrode locations. The function of the colour maps is only for better visualization since all the analyses were performed at the level of single channels. Parametric statistics were adopted after assessing the normality of distribution of the measured variables, by applying the Shapiro–Wilk test, in a population of 12–14 rats during wakefulness. All the variables were tested in a repeated measure design. Thus, principal and interaction effects were tested with one-way or two-way repeated measures ANOVA (rANOVA), in which Greenhouse–Geisser correction was applied when sphericity could not be assumed, while group comparisons were tested with Student's paired-samples *t*-test. Because one channel was removed from the analysis in two rats, two-way ANOVA was used to compare the spatial distribution of variables between left and right hemispheres. Linear fitting was performed with the least-square method. To evaluate correlations and goodness of fit, the coefficient of determination, R^2, was computed and a *t*-test was performed to test the null hypothesis of slope = 0, establishing a *P*-value. When multiple hypotheses were tested across conditions or along cortical areas, the Bonferroni–Holm correction was adopted (number of conditions = 3, corrected $\alpha = 0.01666$; number of cortical areas = 8, corrected $\alpha = 0.00625$ for each hemisphere). Gaussian *υ*-test was used to test volume conduction in connectivity analysis (Cohen 2014; Arena *et al.* 2021). All statistics are two-tailed. The statistical significance in the figures are represented as follows: $P < 0.05$ *, $P < 0.01$ **, $P < 0.001$ ***, $P \geq 0.05$ ns (not significant).

Results

Perturbational complexity was independent of behavioural responsiveness but was reduced by increasing ketamine dosage

In previous studies in humans, ketamine has been found to induce unresponsiveness combined with vivid, dream-like experience, and high cortical complexity (Sarasso *et al.* 2015). Thus, to dissociate cortical complexity from behavioural responsiveness, we recorded spontaneous and evoked EEG activity in six rats, during wakefulness (W) and subsequent constant intravenous infusion of ketamine. We also repeated the electrophysiological experiment with an increased administration rate, to test for a possible dosage dependency. As reported previously (Arena *et al.* 2021), we adjusted the first, low ketamine infusion rate (K1) for every single rat, to the minimal dose that induced behavioural unresponsiveness (i.e. no motor response to pain stimulation). This first dosage, K1, was approximately 1.8 mg/kg/min, iv, while the second subsequent ketamine dose, K2, was set to about two times the first one, at 3.5 mg/kg/min, iv.

During wakefulness, the spontaneous EEG activity was characterized by low amplitude, fast oscillations, typical of cortical activation (Fig. 1a). Interestingly, despite the loss of behavioural responsiveness, the fast oscillations persisted in both K1 and K2 conditions (Fig. 1a), and a general increase of EEG amplitude occurred with ketamine infusion, as shown by the averaged periodogram across channels, which scaled up from wakefulness to K1 and further to the K2 condition (Fig. 1b). In line with this, the mean HF power (20–80 Hz) across channels increased from wakefulness to K1 and further to K2 (Fig. 1c; W: 42.42 ± 0.54 dB, K1: 47.52 ± 0.83 dB, K2: 49.15 ± 0.64 dB; one-way rANOVA, principal effect of condition, $P = 9.1942*10\text{-}8$; paired-samples *t*-test, W vs. K1, $P = 0.0005$, W vs. K2, $P = 6.8217*10^{-5}$, K1 vs. K2, $P = 0.0032$). Likewise, the mean LF (1–4 Hz) power increased from wakefulness to K1 and further to K2 (Fig. 1d; W: 73.57 ± 1.26 dB, K1: 77.75 ± 0.72 dB, K2: 79.75 ± 0.54 dB; one-way rANOVA, principal effect of condition, $P = 0.0021$; paired-samples *t*-test, W vs. K1, $P = 0.0440$, W vs. K2, $P = 0.0271$, K1 vs. K2, $P = 0.0271$). The spectral exponent of the mean periodograms was similar across conditions, indicating a general scaling across all frequencies (Fig. 1e; W: −1.82 ± 0.17, K1: −1.41 ± 0.12, K2: −1.57 ± 0.12; one-way rANOVA, principal effect of condition, $P = 0.1959$; paired-samples *t*-test, W vs. K1, $P = 0.1719$, W vs. K2, $P = 0.3077$, K1 vs. K2, $P = 0.2838$).

Across conditions, the same electrical stimulation induced a similar initial cortical excitation, quantified by the RMS amplitude of the early ERP deflections (Fig. 2a and b; W: 52.63 ± 5.13 μV, K1: 47.65 ± 3.91 μV, K2: 44.84 ± 4.31 μV; one-way rANOVA, principal effect of condition, $P = 0.1943$; paired-samples *t*-test, W vs. K1: $P = 0.2942$, W vs. K2: $P = 0.1613$, K1 vs. K2: $P = 0.1132$). Consistently, the electrical pulse evoked an early, broadband increment in power that was similar across conditions.

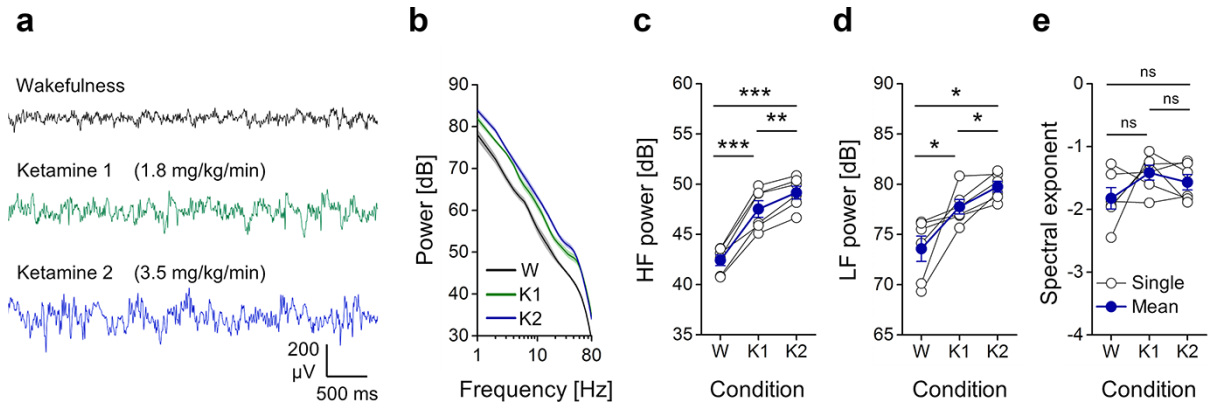

Figure 1. The averaged power spectrum of spontaneous EEG was scaled up from wakefulness to ketamine anaesthesia and by increasing ketamine dosage. (a) Example of spontaneous EEG (5 s) from the retrosplenial/parietal cortex (RS/PA) of one rat during wakefulness (W), light ketamine anaesthesia (ketamine 1, K1; administration rate: 1.8 mg/kg/min i.v.) and deep ketamine anaesthesia (ketamine 2, K2; administration rate: 3.5 mg/kg/min i.v.). (b) Mean periodograms from 16 channels and 6 rats exposed to the same conditions of A (shades represent SEM across rats). (c) Variations of mean high frequency power (HF, 20-80 Hz) and (d) low frequency power (LF, 1-4 Hz) are shown for each rat across conditions and increased from W to K1 and from K1 to K2. (e) The spectral exponents of the averaged periodograms across channels are also reported for each rat and condition

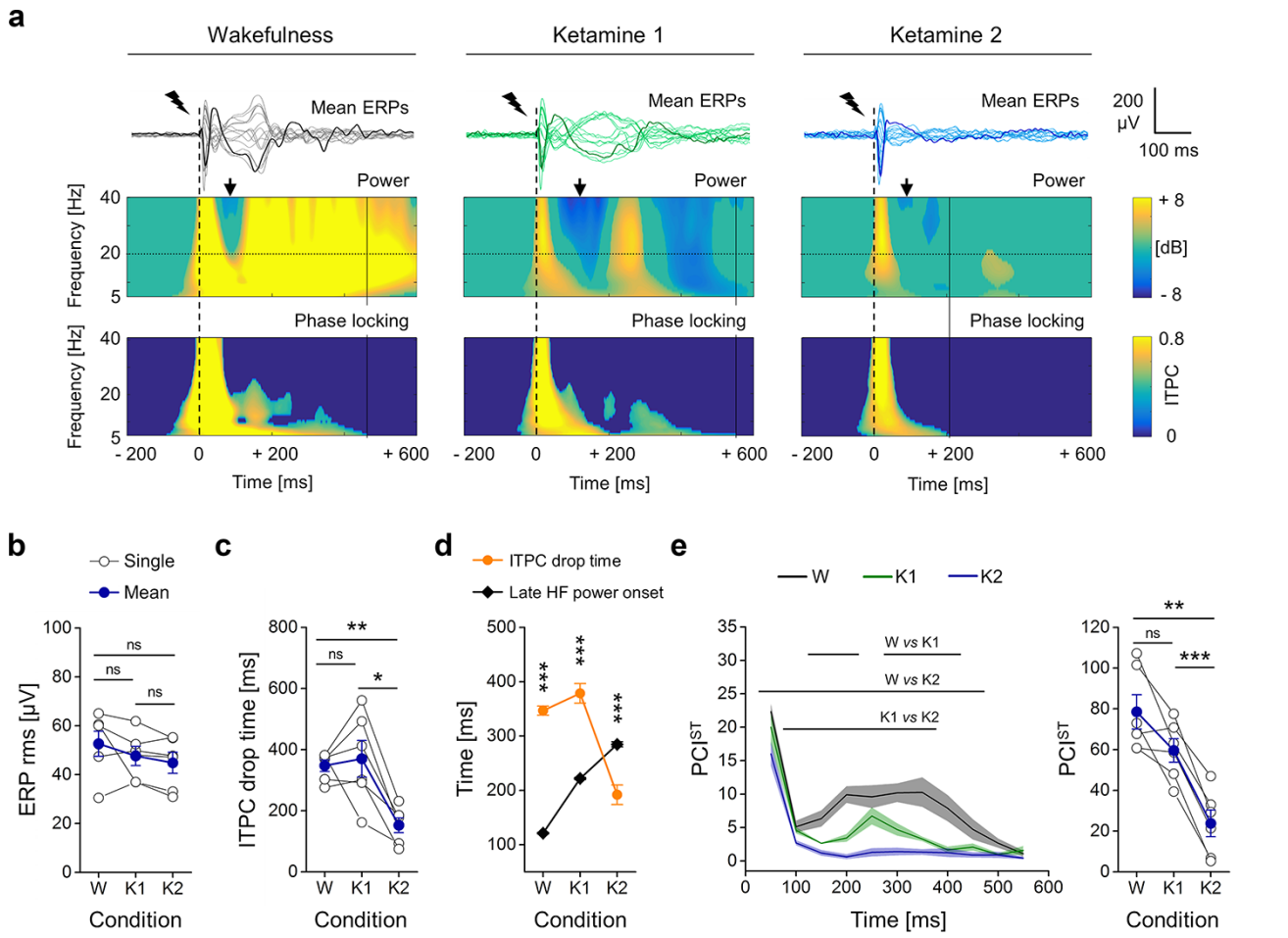

Figure 2. The spatiotemporal dynamics of ERPs revealed a drop in complexity from low to high dosage of ketamine. (a) Top, superimposition of mean ERPs from all 16 electrodes in response to single pulse stimulation (1 ms, 50 µA; dashed line) of the right secondary motor cortex (M2), from the same rat during wakefulness (W, left) and light and deep ketamine anaesthesia (K1, middle and K2, right respectively). One averaged ERP from the same channel over the right primary somatosensory cortex (S1) is in bold for clarity. Middle, power spectrogram (dB) and, bottom, phase-locking across trials (ITPC) from the channel shown in bold above (right S1). The black arrows indicate the moment of relaxation of HF power (dB $\leq$ 0) that follows the first response to stimulation. The ITPC drop time is indicated by vertical continuous lines. (b) The rms amplitude of the early ERP (first 50 ms from stimulus onset) averaged across channels is shown for all rats and conditions. (c) The ITPC drop time (in frequency range 5–80 Hz) averaged across channels is plotted for each rat and condition. (d) The ITPC drop time and the onset of later increased HF power was averaged across channels from all rats and shown for each condition. (e) Left, time courses of mean PCIST (moving windows of 100 ms, 50 ms overlap) and standard errors (shaded) are plotted for all conditions (horizontal lines indicate periods of statistically significant difference between conditions, $P < 0.05$). Right, PCIST in range 0-600 ms is shown for each rat and condition

This activation was quickly followed by a period of relaxation, with HF activity similar to or below the baseline (dB $\leq$ 0), which lasted 150.52 $\pm$ 12.04 ms, averaged across rats and conditions (Fig. 2a, see also Supplementary Fig. S2 for spectrograms and phase-locking plots in the broad frequency range, from 1 to 80 Hz). However, after this first dynamic, the ERP developed differently through time in different conditions. We evaluated the phase consistency of the ERPs across trials, by computing the ITPC at each time point (Cohen 2014; Arena *et al.* 2021) and quantified the duration of the deterministic effect of the stimulus as ITPC drop time (David *et al.* 2006; Pigorini *et al.* 2015; Rosanova *et al.* 2018; Arena *et al.* 2021). During wakefulness and with low ketamine dose, the ERPs showed long-lasting waveforms that were phase-locked across trials, thus still deterministically caused by the stimulation. Conversely, with the high ketamine dosage, the phase-locked response quickly died out, indicated by an earlier ITPC drop, averaged across channels (Fig. 2a and c; W: 347.35 $\pm$ 18.85 ms, K1: 369.76 $\pm$ 59.86 ms, K2: 152.32 $\pm$ 24.17 ms; one-way rANOVA, principal effect of condition, $P = 0.001$; paired-samples *t*-test, W vs. K1: $P = 0.7068$, W vs. K2: $P = 0.0014$, K1 vs. K2: $P = 0.01$). The long-lasting response in wakefulness and K1 also showed a later increase of HF power in most of the channels (W: 100% of channels; K1: 92.36 $\pm$ 4.33% of channels). Such HF activation was largely associated with the deterministic response, since its onset preceded the ITPC drop, as shown by comparing the times of these events from the electrodes with such late increase in HF power (Fig. 2a and d; paired-samples *t*-test, ITPC drop time vs. Late HF power onset; in W: $n = 94$ channels, $P = 7.8199^{*}10^{-45}$; in K1: $n = 87$ channels, $P = 2.6807^{*}10^{-13}$). In contrast, with high ketamine dose, a late HF power activation was still detected in some electrodes (46.6 $\pm$ 14.93% of channels), but was not phase-locked, as it occurred after the ITPC drop (Fig. 2a and d; paired-samples *t*-test, ITPC drop time vs. Late HF power onset, in K2: $n = 44$ channels, $P = 2.1199^{*}10^{-5}$). These results were also associated with an overall reduction of the functional connectivity across channels in the K2 condition, which also corresponded to reduced diversity

of cortical connectivity (Supplementary Fig. S3). Coherently, K2 changed the time course of PCI^{ST}, which was initially high and quickly decayed soon after the stimulation in all conditions. However, in wakefulness and with low ketamine dose, PCI^{ST} built up again, reaching similar values after 200 ms. Then PCI^{ST} dropped again, faster in K1 than W, until fading. Conversely, with high ketamine dose, PCI^{ST} never recovered after the early decay and remained close to 0 (Fig. 2a and e). The time course was in line with the perturbational complexity calculated for the entire response window (0–600 ms), thus PCI^{ST} showed slightly higher values in wakefulness than in K1 condition, but the difference was not statistically significant for this sample [although a significant difference was found for a larger data set (Arena *et al.* 2021), see Discussion]. With a high ketamine dose, however, PCI^{ST} was significantly lower than the other conditions (Fig. 2e; W: 78.47 ± 8.44, K1: 59.57 ± 5.77, K2: 23.75 ± 6.55; one-way rANOVA, principal effect of condition, $P = 4.3026*10^{-5}$; paired-samples t-test, W vs. K1, $P = 0.0535$, W vs. K2, $P = 0.0028$, K1 vs. K2, $P = 0.0005$).

The strong reduction in perturbational complexity was associated with a selective deactivation of bilateral posteromedial cortex

We found that high-dose ketamine caused a non-linear, dose-dependent drop of PCI^{ST} (Fig. 2), but this drop was not associated with a clear overall transition of spontaneous EEG towards slow waves and reduced HF power (Fig. 1). Thus, we investigated the spectral features of spontaneous activity from single cortical areas with higher detail, by computing the local, instantaneous HF/LF ratio (Fernandez *et al.* 2017; Siclari *et al.* 2017; Poulet and Crochet 2018; see Fig. 3a). By averaging across time (from –5 to 0 s) and trials for each electrode, we obtained a topographical distribution of the HF/LF ratio, which was similar between left and right hemispheres, and this symmetry persisted in all conditions (Fig. 3b; two-way ANOVA, principal effect of lateralization, in W: $P = 0.6934$, in K1: $P = 0.9902$, in K2: $P = 0.9789$). By comparing the mean HF/LF ratio across conditions, for each cortical area, we found that it significantly decreased from wakefulness

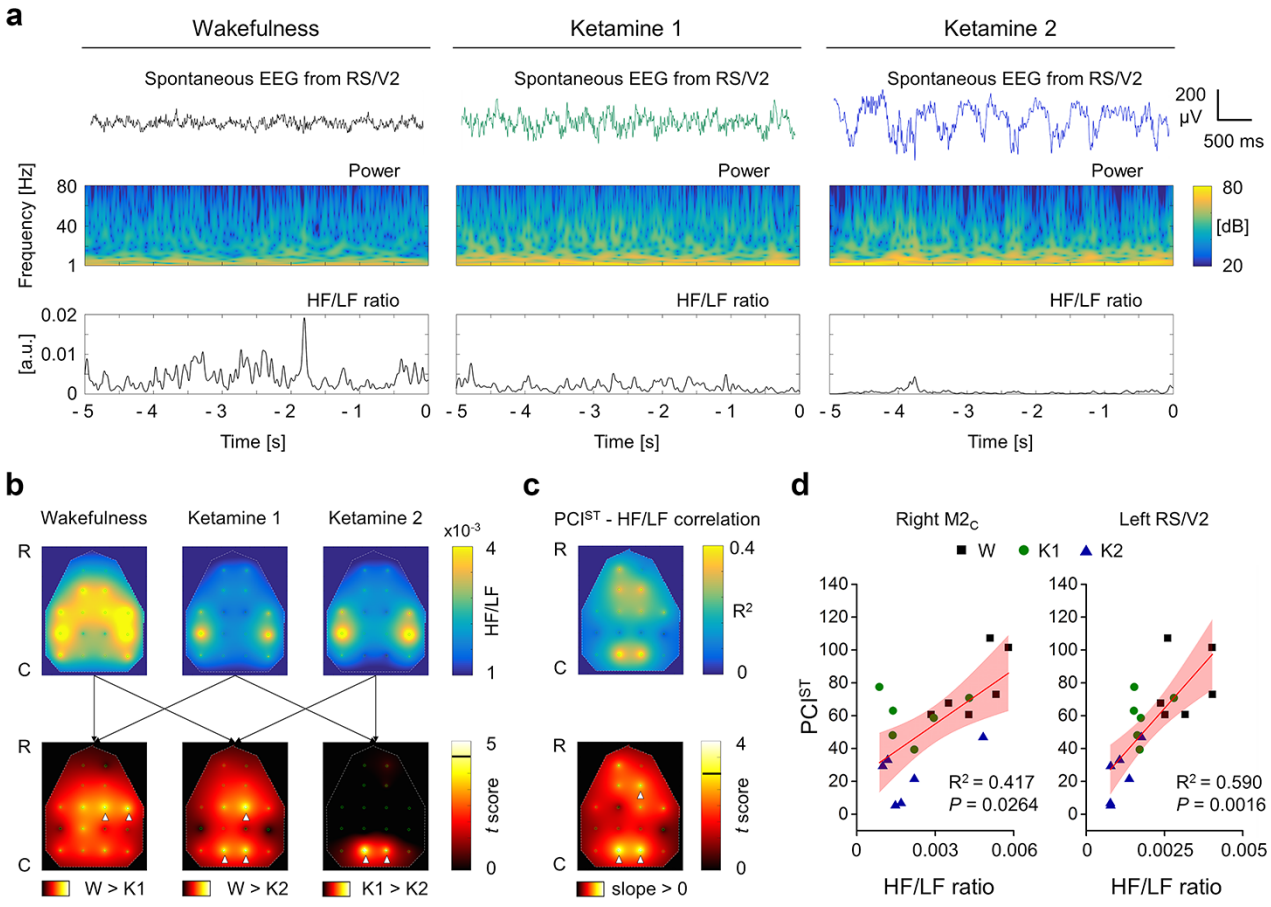

Figure 3. The HF/LF ratio of spontaneous EEG in bilateral posteromedial cortex was selectively reduced by increasing ketamine dosage and correlated with the level of PCIST. (a) Up, Example of spontaneous EEG (5 s) from the posteromedial cortex (RS/V2) of one rat during wakefulness (W), light ketamine anaesthesia (ketamine 1, K1) and deep ketamine anaesthesia (ketamine 2, K2) and below, the relative spectrogram and the ratio between high frequency (HF, 20–80 Hz) and low frequency (LF, 1–4 Hz) powers (HF/LF ratio) in time. (b) The colour maps show the topographical distributions (R-C: rostral-caudal) of the 16 EEG electrodes (small green circles) and, above, the spatial interpolations of the HF/LF ratio, averaged across time, trials and rats, for each condition. Below, the colour maps report the spatial interpolation of the *t*-scores (paired-samples *t*-test) from comparing the HF/LF ratio across conditions for each channel (left, wakefulness vs. ketamine 1; middle, wakefulness vs. ketamine 2; right, ketamine 1 vs. ketamine 2). The horizontal black line in the colour bar indicates the threshold for statistical significance (t5 = 4.5258, Bonferroni–Holm corrected). White arrowheads indicate the channels with statistically significant differences across conditions. (c) Above, the colour map shows the spatial distribution of the coefficient of determination R2 from the correlation between PCIST and HF/LF ratio, across rats and conditions, for each channel. Below, the colour map reports the spatial interpolation of *t*-scores, assessing the statistical significance of the correlation for each channel. The horizontal black line in the colour bar indicates the threshold for statistical significance (t16 = 3.1458, Bonferroni–Holm corrected). White arrowheads indicate the channels showing statistically significant correlations. The correlations of right M2C and left RS/V2 are reported in (d) with respective R2 and *P*-values

to low ketamine dosage only in right M2/M1 cortex (HF/LF*10^{-3}, paired-samples *t*-test; W: 4.28 ± 0.60, K1: 1.13 ± 0.25, $P = 0.0372$) and S1 cortex (HF/LF*10^{-3}, paired-samples *t*-test; W: 6.48 ± 0.69, K1: 3.48 ± 0.51, $P = 0.0372$), although weak, non-significant reductions were also seen elsewhere (Fig. 3b). In contrast, high doses of ketamine selectively reduced the mean HF/LF ratio in the bilateral posteromedial cortex (left and right RS/V2 channels), indicating a specific deactivation of this part of the cortex, with respect to the K1 condition (Fig. 3a and b, Supplementary Fig. S4; left RS/V2, HF/LF*10^{-3}, paired-samples *t*-test; K1: 1.82 ± 0.19, K2: 1.09 ± 0.17, $P = 0.0088$; right RS/V2, HF/LF*10^{-3}, paired-samples *t*-test; K1: 1.50 ± 0.20, K2: 0.91 ± 0.14, $P = 0.0431$). In line with these results, the HF/LF ratios at both bilateral RS/V2 and right M2/M1 cortex were also reduced from wakefulness to the K2 condition (Fig. 3b). To test whether the level of activation of any cortical area was effectively able to predict the complexity of global cortical dynamics, we assessed possible regional correlations between HF/LF ratio and PCI^{ST} (Fig. 3c). We found that the HF/LF ratio from the spontaneous activity of bilateral posteromedial cortex (left, right RS/V2) was highly, linearly correlated with the PCI^{ST} value across conditions (Fig. 3c and d; left RS/V2: linear fit, $R^2 = 0.590$, $P = 0.0016$; right RS/V2: linear fit, $R^2 = 0.568$, $P = 0.0024$). A weaker but significant correlation was also identified only at the level of the right secondary motor cortex (Fig. 3c and d; right $M2_C$: linear fit, $R^2 = 0.417$, $P = 0.0264$).

Next, we assessed the same correlations between local HF/LF ratio and global PCI^{ST}, this time distinguishing between brain states and state transitions. We first evaluated the correlation in wakefulness condition alone, where both behavioural responsiveness and high perturbational complexity were present (Fig. 4a and b; data from three different recordings, performed in three different days on the same rats were considered only in this condition, to increase the number of observations). Then, we repeated the estimation of the correlations by considering the conditions of wakefulness and low dosage of ketamine, when perturbational complexity is still high, but behaviour transitions from responsiveness to unresponsiveness (Fig. 4c and d). Finally, we evaluated the correlations in conditions of low and high ketamine dosages, when only the variation of perturbational complexity occurred, within the same unresponsive behavioural state (Fig. 4e and f). With this, we attempted to identify possible roles that specific cortical regions might have in specific state transitions. Within the wakefulness condition, we could not identify any significant correlation between PCI^{ST} and HF/LF ratio at the level of any cortical area. Nevertheless, the correlations with higher R^2, which were also closer to the threshold for statistical significance, seemed to be clustered in the secondary motor cortex (Fig. 4a and b; right $M2_C$: linear fit, $R^2 = 0.377$, $P = 0.0538$; left RS/V2: linear fit, $R^2 = 0.077$, $P = 1$). Likewise, the HF/LF ratio could not clearly predict PCI^{ST} between wakefulness and low ketamine dose, when only behavioural responsiveness changed, for any of the cortical areas (Fig. 4c and d; right $M2_C$: linear fit, $R^2 = 0.386$, $P = 0.2173$; left RS/V2: linear fit, $R^2 = 0.271$, $P = 0.4124$). On the other hand, by considering only the variations induced by increasing ketamine dosage (K1 and K2), we found a significant and strong correlation selectively associated with the left RS/V2 cortex, thus indicating that the state of activation or deactivation of the posteromedial cortex could effectively linearly predict the complexity level of the entire cortical network and its breakdown (Fig. 4e and f; right $M2_C$: linear fit, $R^2 = 0.064$, $P = 0.1$; left RS/V2: linear fit, $R^2 = 0.568$, $P = 0.0370$). Coherently with these results, by considering only the conditions of wakefulness and high dose of ketamine, the variation of behavioural responsiveness could not be separated from changes in perturbational complexity, hence a significant correlation between PCI^{ST} and the HF/LF ratio was detected in both frontal cortex and posteromedial cortex (Supplementary Fig. S5).

In principle, the reduction of the HF/LF ratio can be determined by an increase of LF powers, by a decrease of HF powers, or by a combination of the two events. Thus, in order to explain the reduction seen in the posteromedial cortex, we assessed the LF and HF powers at the level of each cortical area, across conditions (Fig. 5a). At first, we tested for possible lateralization, without finding any clear difference between left and right hemispheres in each experimental condition, for both LF powers (Fig. 5a; two-way ANOVA, principal effect of lateralization, in W: $P = 0.7581$, in K1: $P = 0.9459$, in K2: $P = 0.9589$;), as well as for HF power (Fig. 5a; two-way ANOVA, principal effect of lateralization, in W: $P = 0.8284$, in K1: $P = 0.9664$, in K2: $P = 0.6748$). However, LF powers were differentially distributed across cortical areas, and an overall increase in power could be detected in relation to the increment of ketamine dosage (Fig. 5b; two-way rANOVA, principal effect of cortical areas: $P = 0.0009$, principal effect of ketamine dosage: $P = 0.0132$). Similar effects were also found for HF powers (Fig. 5b; two-way rANOVA, principal effect of cortical areas: $P = 0.0109$, principal effect of ketamine dosage: $P = 0.0041$), and were in line with the scaling up of the mean periodograms, seen by averaging across electrodes (Fig. 1). Nevertheless, by comparing powers between K1 and K2 conditions for every single channel, a significant increase of LF power was only found at the level of bilateral posteromedial cortex (left and right RS/V2), while the increase of HF power was more spatially sparse, without a clear clusterization (Fig. 5b). To more directly compare the relative increment of powers that occurred by increasing ketamine dosage, we computed the ratio between K2 and K1 conditions (K2/K1), for both HF and LF powers, at the level of each cortical area (Fig. 5c). Overall, the power increments were differentially distributed across cortical areas, and an overall difference between HF and LF could not be detected (Fig. 5c; two-way rANOVA, principal effect of cortical areas: $P = 0.0325$, principal effect of frequency range: $P = 0.0744$). However, a clear interaction effect between cortical areas and frequency ranges was identified (Fig. 5c; two-way rANOVA, interaction effect: $P = 0.0056$), thus indicating the relation between the increments of HF and LF powers changed depending on the specific cortical area. Indeed, LF power increased significantly more than HF power selectively in the bilateral posteromedial cortex (left and right RS/V2), conversely, HF power had the tendency to increase more than LF power in parieto-frontal areas, even if without reaching statistical significance (Fig. 5c).

Discussion

We reanalysed multichannel EEG data from wakefulness (W) and two levels of ketamine anaesthesia (K1, K2) in rats, based on previous experiments (Arena *et al.* 2021). To assess the capacity for consciousness in each state, we computed PCI^{ST} (Comolatti *et al.* 2019) and compared these results to region-specific estimates of cortical activation, assessed by HF/LF ratio of spontaneous EEG activity for each electrode (Fernandez *et al.* 2017; Siclari *et al.* 2017; Poulet and Crochet 2018).

In humans, ketamine anaesthesia has been observed to induce a dissociated state of behavioural unresponsiveness with dream-like, vivid conscious experiences (Collier 1972; Sarasso *et al.* 2015). We took advantage of this and used a controlled intravenous infu-

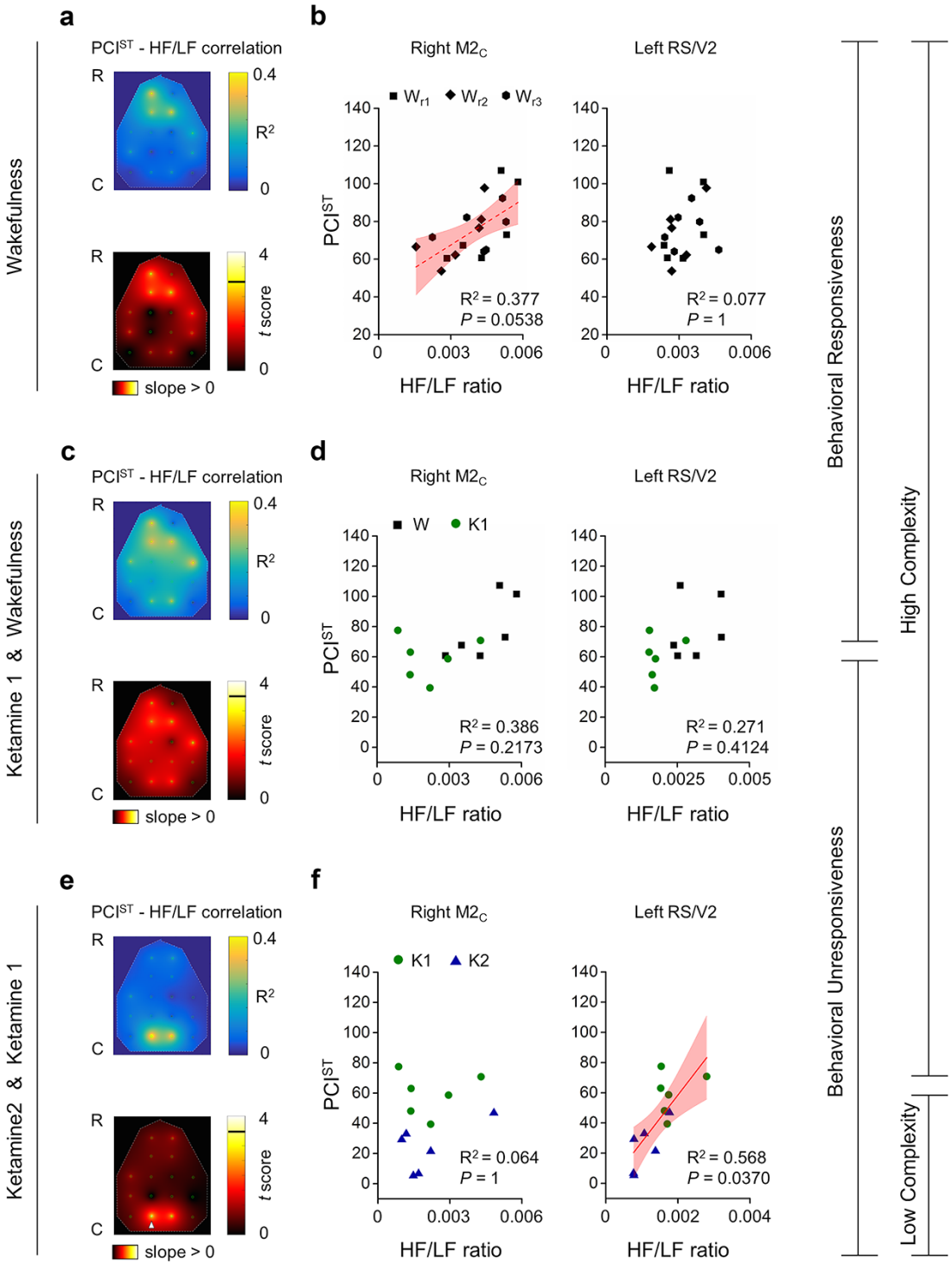

Figure 4. HF/LF ratio of spontaneous EEG from posteromedial cortex selectively correlated with PCIST in conditions of behavioural unresponsiveness, with light and high ketamine anaesthesia. (a, b) The putative correlations between PCIST and HF/LF ratio are shown in wakefulness across rats and 3 recording sessions (Wr1 Wr2 Wr3), during the presence of both behavioural responsiveness and high cortical complexity. (c, d) The same putative correlations are shown across rats and across conditions of wakefulness (W) and low ketamine anaesthesia (K1), when loss of behavioural responsiveness occurred, but high cortical complexity persisted. (e, f) Correlations between PCIST and HF/LF ratio are also computed and shown across rats and across conditions of low and high ketamine doses (K1 and K2, respectively) when reduction of cortical complexity occurred and behavioural unresponsiveness was unchanged. In panels A, C, E the colour maps show the spatial interpolation of R2 and *t*-scores (above and below respectively, for all panels) from the correlations of all channels. The horizontal black line in the colour bar indicates the threshold for statistical significance. The white arrowhead indicates channels with statistically significant correlation between PCIST and HF/LF ratio. In panels B, D, F the correlations and/or absence of correlation of right secondary motor cortex (M2C, left side of the panel) and left posteromedial cortex (RS/V2, right side of the panel) are reported with relative R2 and *P*-values, (corrected for multiple comparisons). Dashed line is used to indicate a correlation close to statistical significance (panel B, left), while a continuous line indicates a statistically significant linear fitting and correlation (panel F, right)

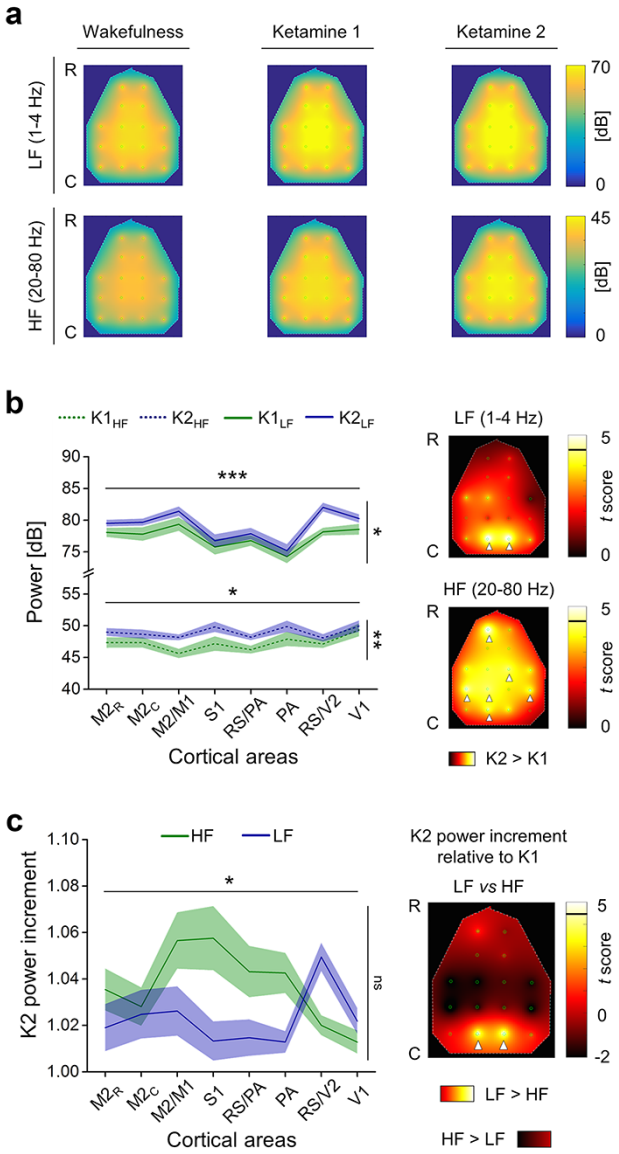

Figure 5. The reduction of HF/LF ratio from low to high dosage of ketamine in the posteromedial cortex was explained by a selective higher increment of LF powers with respect to HF. (a) The colour maps show the topographical distributions (R-C: rostral-caudal) of the 16 EEG electrodes (small green circles) and the spatial interpolations of the LF power (1–4 Hz, above) and HF power (20–80 Hz, below), averaged across time, trials and rats, for each condition. (b) Left, averaged HF (dashed line) and LF (continuous line) powers across hemispheres and rats are shown for each cortical area, during both low and high ketamine dosage (K1 and K2, respectively). On the right, the colour maps show the spatial interpolation of *t*-scores from comparing LF powers (up) and HF powers (bottom) between K1 and K2 conditions, for each channel. The horizontal black lines in the colour bar indicate the threshold for statistical significance (t5 = 4.5258, Bonferroni–Holm corrected). White arrowheads indicate channels with statistically significant differences across conditions. (c) Left, the ratio between low and high doses of ketamine is reported for both HF and LF powers at the level of each cortical area, thus showing the power increments induced by deep ketamine anaesthesia (K2). Right, spatial interpolation of the *t*-scores from comparing LF power increment with HF power increments induced by increasing ketamine dosage, for each channel. The horizontal black line in the colour bar indicates the threshold for statistical significance (t5 = 4.5258, Bonferroni–Holm corrected). White arrowheads indicate the channels with statistically significant differences between the two frequency ranges

sion of ketamine to dissociate the capacity for consciousness from responsiveness. In agreement with a PCI study in humans (Sarasso *et al.* 2015), we found that PCI^{ST} was not significantly changed during the unresponsive state caused by light ketamine anaesthesia (K1) compared to wakefulness (Fig. 2), even if it tended to be lower in the K1 condition. This tendency is more in line with results from a larger dataset from rats (Arena *et al.* 2021) and in agreement with the time course of PCI^{ST}, which showed both periods of similarities and differences between wakefulness and light ketamine anaesthesia. The difference in the statistical significance of the PCI^{ST} values reported here compared to previous experiments (Arena *et al.* 2021) might be due to the smaller sample size here. However, in both W and K1 conditions, PCI^{ST} built up again after an initial decay, reaching similar values between 200 and 300 ms after the stimulus onset (Fig. 2). Indeed, our results support the idea that high perturbational complexity is associated with a capacity to sustain long-lasting sequences of deterministic activations (Mukovski *et al.* 2007; Pigorini *et al.* 2015; Rosanova *et al.* 2018; Arena *et al.* 2021) as shown by the long-lasting phase-locked cortical ERPs (Fig. 2) and by the strong yet diverse global connectivity observed here (Supplementary Fig. S3). Moreover, the widespread responses to stimulation required for high PCI^{ST}

may also indicate a capacity for the kind of global broadcasting required for consciousness according to GNW (Mashour *et al.* 2020), as well as for the brain to function as an integrated and differentiated whole as is required for consciousness in IIT (Casali *et al.* 2013; Tononi *et al.* 2016). Although a partially reduced level of consciousness might be inferred from the tendency of PCI^{ST} to be lower with light ketamine anaesthesia compared to wakefulness, we observed relatively high spatiotemporal complexity during both conditions, with long-lasting and well-integrated phase-locked cortical activations. Thus, taken together, our findings are compatible with a fully, or at least partially, preserved capacity for consciousness during both wakefulness and light ketamine anaesthesia, independently of behavioural responsiveness.

However, ketamine has also been shown to produce fluctuations between high and low spatiotemporal complexity of spontaneous EEG in humans, following bolus injection of an anaesthetic dose (Li and Mashour 2019). This phenomenon may be caused by the unstable pharmacokinetic of the bolus injection, suggesting a dose-dependent effect. Consistently, it was reported that soon after bolus injection, when ketamine plasma level is high, the spontaneous EEG can assume a gamma-burst dynamic, with slow oscillations that interrupted an enhanced HF, gamma activity (Akeju *et al.* 2016). Conversely, when ketamine plasma level was reduced, about 10 min after bolus injection, the spontaneous EEG activity was characterized by uninterrupted, stable gamma/beta activity, with reduced slow frequency power (Akeju *et al.* 2016), and the spatiotemporal complexity of spontaneous EEG stabilized at wakefulness-like values (Li and Mashour 2019). Importantly, the spatiotemporal complexity of the thalamocortical system is thought to be a promising neuronal correlate for the capacity for consciousness (Tononi and Edelman 1998; Dehaene 2014; Koch *et al.* 2016; Sarasso *et al.* 2021), and was empirically found to correlate with conscious experience, in both spontaneous (Ferenets *et al.* 2006; Schartner *et al.* 2015; Demertzi *et al.* 2019) and perturbed activity (Massimini *et al.* 2009; Casali *et al.* 2013; Sarasso *et al.* 2015; Casarotto *et al.* 2016; Rosanova *et al.* 2018; Comolatti *et al.* 2019). Thus, it is conceivable that low and high doses of ketamine, although both cause behavioural unresponsiveness, may still induce quite different states of consciousness: the low dose may allow vivid but covert dream-like experiences to occur (Collier 1972; Sarasso *et al.* 2015), while the high dose may cause dreamless unconsciousness, due to different, dose-dependent effects on cortical complexity (Li and Mashour 2019).

We tested this hypothesis by repeating the same electrophysiological recording/stimulations in the same rats during the constant intravenous infusion of ketamine at a higher rate, which gives a more constant systemic concentration than with bolus injection. In this high-dose condition (K2), we found that PCI^{ST} was strongly reduced along with an earlier interruption of phase-locked response (Fig. 2) and with a drastic reduction of cortical functional connectivity and diversity (Supplementary Fig. S3). These results are compatible with a reduced capacity to integrate or broadcast information within the global cortical network, thus suggesting a reduced capacity for consciousness during deep ketamine anaesthesia (K2). This also indicates a clear dose-dependent effect, which was only suggested by previous experiments (Akeju *et al.* 2016; Li and Mashour 2019). In agreement with Li and Mashour (2019), our results demonstrate that ketamine anaesthesia can be used to dissociate behavioural responsiveness from cortical complexity, thus representing a 'unique tool to probe different states of consciousness' (Li and Mashour 2019). This is in contrast to other general anaesthetics, for which behavioural responsiveness and capacity for consciousness seem more strongly connected and difficult to dissociate (Sarasso *et al.* 2015; Arena *et al.* 2021).

Next, we explored the spectral properties of ongoing cortical activity in order to identify possible associations with the different combinations of behavioural responsiveness and capacity for consciousness, as assessed by PCI^{ST} (Comolatti *et al.* 2019). The spontaneous EEG activity during ketamine anaesthesia was characterized by a widespread, dose-dependent increase in HF power compared to wakefulness (Figs 1 and 5), in agreement with previous findings (Maksimow *et al.* 2006; Akeju *et al.* 2016; Li and Mashour 2019). HF oscillations are usually associated with neuronal firing (Steriade *et al.* 1996, 2001; Mukovski *et al.* 2007) and cortical activation (Fernandez *et al.* 2017; Siclari *et al.* 2017; Poulet and Crochet 2018). Thus, the observed increase in HF power is consistent with the enhanced presynaptic release occurring after ketamine administration (Ferro *et al.* 2017), and with the idea that ketamine, via its antagonism of NMDA receptors, might mainly inhibit GABAergic interneurons, producing a state of overall cortical excitation (Seamans 2008). Interestingly, LF power also increased from wakefulness to ketamine anaesthesia in a dose-dependent manner (Figs 1 and 5), in agreement with previous reports (Akeju *et al.* 2016; Li and Mashour 2019). Thus, ketamine induced a scaling up of the entire power spectrum of the spontaneous EEG, suggesting a maintained balance between the inhibition and excitation of the overall cortical network underlying the EEG signal (Gao *et al.* 2017). This was supported by the observation of a similar spectral exponent across conditions (Fig. 1), which has been hypothesized to indicate an aroused or conscious state (Colombo *et al.* 2019; Lendner *et al.* 2020; Arena *et al.* 2021). Why then did we observe the strong reduction of PCI^{ST} in the transition from low to high ketamine condition (Fig. 2)?

One hypothesis is that specific cortical circuits might be particularly relevant for sustaining complex neuronal interactions and that the activation state of these circuits might diverge from the average dynamic of the entire cortical network. Indeed, it is known that transient and local cortical deactivations or activations can occur and dissociate from the global brain state, such as with local sleep during wakefulness (Murphy *et al.* 2011; Vyazovskiy *et al.* 2011; Fernandez *et al.* 2017), possibly modifying the capacity for behaviour and/or conscious experience (Vyazovskiy *et al.* 2011; Fernandez *et al.* 2017; Siclari *et al.* 2017; Poulet and Crochet 2018). For example, it has been shown that localized reduction of LF power and increased HF activity (high HF/LF ratio) within the posterior cortex is strongly associated with dream experience in humans during deep stages of sleep (Siclari *et al.* 2017), a state dominated by LF activity that is often linked to unconsciousness (Tononi and Massimini 2008). Thus, to uncover the role and the state of activation of specific areas, we similarly measured the HF (20–80 Hz)/LF (1–4 Hz) power ratio from the spontaneous activity of all the 16 epidural electrodes and compared across experimental conditions.

Although both light and deep ketamine anaesthesia caused an unresponsive behavioural state, we were able to identify regional variations in HF/LF ratio that were related to changes in the global PCI^{ST} value. Strikingly, the bilateral posteromedial cortex was the only region that showed a consistent reduction of HF/LF ratio, from low to high ketamine dosage, along with the drop in PCI^{ST} (Fig. 3). The reduced ratio within the posteromedial cortex indicated a local deactivation (Poulet and Crochet 2018), which was explained by a larger increase of LF than HF power induced by the increased ketamine dosage (Fig. 5). This local power imbalance might indicate a particularly pronounced gamma-burst activity

pattern (Supplementary Fig. S4), typical of high ketamine plasma levels, with slow waves interrupting enhanced HF activity (Akeju et al. 2016; Li and Mashour 2019). Consistently, the HF/LF ratio over the posteromedial cortex strongly correlated with the PCI^{ST} level during ketamine administration (Fig. 4) and across all conditions (Fig. 3), but not within wakefulness alone or between wakefulness and light ketamine anaesthesia (Fig. 4), where PCI^{ST} did not change substantially. These results indicate that the local state of the RS/V2 cortex is associated with the capacity for long-lasting, broadly integrated and differentiated cortical activations as assessed by PCI^{ST}. Thus possibly, the posteromedial cortex may play an important role in sustaining the capacity for consciousness, in a general agreement with both IIT and GNW (Tononi et al. 2016; Mashour et al. 2020). In other words, our results may support the hypothesis that a selective deactivation of the posteromedial cortex—as indicated by the localized decrease in HF/LF power—is correlated with, and may even underlie, a sharp reduction of the brain's capacity to globally broadcast information or to function as an integrated and differentiated whole that is capable of sustaining consciousness. This is complementary to the occurrence of dreaming during deep stages of sleep in humans, which was associated with reduced LF activity and increased HF power in posterior cortical areas, indicating a local cortical activation [high HF/LF ratio, (Siclari et al. 2017)]. Moreover, our findings are consistent with the reduced functional integration and diversity that was seen in the posterior regions of the brain's default mode network during unconsciousness, in humans (Luppi et al. 2019).

In contrast, light ketamine anaesthesia produced a significant reduction of HF/LF ratio compared to wakefulness only over the right primary motor and somatosensory cortex (Fig. 3). This was consistent with the loss of behavioural responsiveness induced by the low ketamine dose, and possibly with an analgesic effect. A correlation between the HF/LF ratio of the right secondary motor cortex and PCI^{ST} was also found across conditions (Fig. 3). However, this relation was at least partially explained by a wakefulness-specific weak correlation (Fig. 4), which could reflect behavioural variations within the same state, such as active/quiet wakefulness or transient attentional loading. These findings are indeed consistent with the connection between the prefrontal cortex and behavioural state, which was recently demonstrated by local cortical injections of carbachol, during general anaesthesia, in rats (Pal et al. 2018). In these experiments, during sevoflurane anaesthesia, local cholinergic modulation of both associative frontal and parietal cortices produced a transition from slow-wave EEG activity to low voltage, wakefulness-like, fast oscillations (Pal et al. 2018). EEG temporal complexity also increased with both local cortical activations (Pal et al. 2020). However, only the cholinergic activation of the prefrontal cortex was able to restore wakefulness-like motor activity (Pal et al. 2018), showing how cortical complexity can be effectively dissociated from behaviour (Pal et al. 2020). Unfortunately, PCI was not tested, and the state of consciousness was only inferred by the simple motor activity (Pal et al. 2018, 2020), while it is known that these phenomena can dissociate in humans, under several circumstances (Blumenfeld 2005; Owen et al. 2006; Ghoneim et al. 2009; Noreika et al. 2011; Castelnovo et al. 2018; Linassi et al. 2018).

In our experimental setting, the electrodes over the posteromedial cortex cover both the medial part of the secondary visual cortex and the caudal part of the retrosplenial cortex (Supplementary Fig. S1). Interestingly, the dose-dependent deactivation of this cortical region is reminiscent of a recent finding, in which sub-anaesthetic bolus injections of ketamine were found to induce slow-wave oscillations and synchronized, rhythmic neuronal silencing selectively in the retrosplenial cortex in mice, affecting behaviour (Vesuna et al. 2020). The retrosplenial cortex is a particularly highly integrated area, within the medial cortical subnetwork of rodents (Zingg et al. 2014). It receives information from the claustrum, indirectly from the hippocampus through the subiculum, and it is directly interconnected with several sensory areas (visual, auditory, and somatosensory) and high-order associative areas, including the medial frontal cortex. Thus, it is likely to play important roles in multisensory integration and also integration with higher functions such as episodic memory, spatial navigation, and motor planning (Zingg et al. 2014). Given this, it is not surprising that deactivation of this area (low HF/LF ratio, Fig. 3), due to enhanced LF activity (Fig. 5), could be associated with disruption of widespread integration of complex cortical interactions as seen here, with the drop of PCI^{ST} at high ketamine dosage (Fig. 2). In other words, there is reason to believe that the specific deactivation of a region in the posteromedial cortex can be directly involved in breaking down the properties required for sustaining a capacity for consciousness. However, the associative frontal cortex is also highly integrated (Zingg et al. 2014; Barthas and Kwan 2017) and several pieces of evidence suggest its involvement in conscious processing (Del Cul et al. 2009; Kapoor et al. 2020; Weilnhammer et al. 2021; Levinson et al. 2021). Moreover, our results cannot exclude that a selective inhibition or lesioning of M2, within a global activated state, could also disrupt cortical complexity. Thus, in future experiments, it will be important to causally control the state of activation of single cortical areas, with local intervention, in combination with PCI^{ST}, to better address the role of specific cortical regions in sustaining the capacity for consciousness.

The main findings presented here are compatible with several theories of consciousness, as it is widely agreed that some sort of long-range interactions within the brain are required to sustain its capacity for consciousness. For example, GNW requires information to be globally broadcast (Baars 2005; Dehaene et al. 2011; Mashour et al. 2020), IIT requires the physical substrate of consciousness to be integrated (Tononi and Edelman 1998; Tononi et al. 2016), and at least some higher-order theories require long-range interaction to maintain the capacity to form representations in associative cortices about first-order states in early sensory regions (Lau and Rosenthal 2011; Brown et al. 2019). Nonetheless, our results suggest that the kind of global cortical complexity associated with conscious experience breaks down when ketamine specifically deactivates the posteromedial cortex (Figs 3 and 4). Moreover, the finding that the ketamine-induced deactivation of primary motor and somatosensory cortex was associated with loss of behavioural responsiveness, but not with significant changes in PCI^{ST} (see Fig. 3), or in durable and well-integrated cortical activations (Fig. 3, Supplementary Fig. S3), seems to provide an example that some cortices may be deactivated without disrupting the normal capacity for consciousness. Thus, theories of consciousness should be able to explain why some regions may be deactivated without any apparent effect on the brain's overall capacity for consciousness, while others are more critical. We also observed that changes in the HF/LF ratio of secondary motor regions during wakefulness had a tendency of correlating with changes in PCI^{ST} (Fig. 4). This weak relation may represent a modulatory effect of frontal regions on the overall capacity for consciousness during wakefulness. As these variations did not result from controlled intervention, they suggest that spontaneous changes in frontal activity (HF/LF),

likely involving changes in related cognitive functions [working memory, attention, cognitive control, planning, decision-making, etc.; (Dalley *et al.* 2004)], might reflect spontaneous modulation of cortical complexity within limits of normal wakefulness. This seems to be compatible with theories of consciousness that also attribute an active role to the frontal cortices of selectively modulating the contents of consciousness and attention at any given moment (Baars 2005; Dehaene *et al.* 2011; Lau and Rosenthal 2011; Helfrich *et al.* 2018; Brown *et al.* 2019; Mashour *et al.* 2020).

Of course, these findings are not conclusive, as the specific regional changes in HF/LF observed are dependent on fluctuations in ongoing activity as opposed to interventional inactivation. Furthermore, it is not necessarily the case that the changes in HF/LF observed in different regions were caused by the same underlying processes, and it is also uncertain that they were always indicative of a deactivation of the region. To address these issues, we aim for future experiments with controlled, direct inactivation of individual cortical regions while measuring PCI^{ST} from awake rodents.

Conclusion

By comparing EEG in light and deep ketamine anaesthesia in rats, we dissociated changes in global and local cortical dynamics related to loss of behavioural responsiveness from those likely related to capacity for consciousness (assessed by PCI^{ST}). Light ketamine anaesthesia induced an unresponsive state with apparent deactivation of primary somatosensory and motor regions (indicated by locally reduced HF/LF power ratio). The mean PCI^{ST} value was somewhat lower than in wakefulness, but long-lasting phase-locked responses with high and diversified functional connectivity suggested a dissociated state, with largely conserved consciousness. In contrast, deep ketamine anaesthesia strongly reduced PCI^{ST}, with early interruption of phase-locked response and disruption of functional connectivity, suggesting a more fully unconscious state. The latter was associated with highly selective deactivation of the posteromedial cortex, which was not seen during light ketamine anaesthesia, suggesting a significant role for this cortical region in the capacity for consciousness.

Supplementary data

Supplementary data is available at *NCONSC* online.

Data availability

Data will be available in the public repository EBRAINS upon publication at the following DOIs: 10.25493/S0DM-BK5; 10.25493/E9EF-6SB.

Funding

This project/research received funding from the European Union's Horizon 2020 Framework Programme for Research and Innovation under the Specific Grant Agreements No. 945539 (Human Brain Project SGA3, JFS), No. 785907 (Human Brain Project SGA2; JFS), and No. 720270 (Human Brain Project SGA1; JFS).

Author contributions

A.A. designed the experiments; A.A., S.T. performed experiments and collected data; A.A. analysed data; R.C. performed PCIST analysis; A.A., B.E.J., J.F.S. wrote the manuscript; all authors participated in the interpretation of results and revision of the manuscript, and approved the final version of the manuscript.

Conflict of interest statement

The authors declare that they have no financial competing interests.

References

Akeju O, Song AH, Hamilos AE *et al.* Electroencephalogram signatures of ketamine anesthesia-induced unconsciousness. *Clin Neurophysiol* 2016;**127**:2414–22.

Arena A, Comolatti R, Thon S *et al.* General anesthesia disrupts complex cortical dynamics in response to intracranial electrical stimulation in rats. *eNeuro* 2021;**8**:4.

Arena A, Thon S, Storm J. PCI-like measure in rodents. *Hum Brain Project Neuroinf Platform* 2019.

Baars BJ. Global workspace theory of consciousness: toward a cognitive neuroscience of human experience. In: Laureys S (ed.), *The Boundaries of Consciousness: Neurobiology and Neuropathology*. Amsterdam: Elsevier, 2005, 45–53.

Barthas F, Kwan AC. Secondary motor cortex: where "sensory" meets "motor" in the rodent frontal cortex. *Trends Neurosci* 2017;**40**:181–93.

Blumenfeld H. Consciousness and epilepsy: why are patients with absence seizures absent? *Prog Brain Res* 2005;**150**:271–86.

Boly M, Massimini M, Tsuchiya N *et al.* Are the neural correlates of consciousness in the front or in the back of the cerebral cortex? Clinical and neuroimaging evidence. *J Neurosci* 2017;**37**:9603–13.

Brown EN, Lydic R, Schiff ND. General anesthesia, sleep, and coma. *N Engl J Med* 2010;**363**:2638–50.

Brown R, Lau H, LeDoux JE. Understanding the higher-order approach to consciousness. *Trends Cogn Sci* 2019;**23**:754–68.

Casali AG, Gosseries O, Rosanova M *et al.* A theoretically based index of consciousness independent of sensory processing and behavior. *Sci Transl Med* 2013;**5**:198ra105.

Casarotto S, Comanducci A, Rosanova M *et al.* Stratification of unresponsive patients by an independently validated index of brain complexity. *Ann Neurol* 2016;**80**:718–29.

Castelnovo A, Lopez R, Proserpio P *et al.* deep stages of sleep parasomnias as disorders of sleep-state dissociation. *Nat Rev Neurol* 2018;**14**:470–81.

Chernik DA, Gillings D, Laine H *et al.* Validity and reliability of the Observer's Assessment of Alertness/Sedation Scale: study with intravenous midazolam. *J Clin Psychopharmacol* 1990;**10**:244–51.

Cohen MX. *Analyzing Neural Time Series Data: Theory and Practice*. 1 edn. Cambridge, MA: MIT Press, 2014.

Collier BB. Ketamine and the conscious mind. *Anaesthesia* 1972;**27**:120–34.

Colombo MA, Napolitani M, Boly M *et al.* The spectral exponent of the resting EEG indexes the presence of consciousness during unresponsiveness induced by propofol, xenon, and ketamine. *NeuroImage* 2019;**189**:631–44.

Comanducci A, Boly M, Claassen J *et al.* Clinical and advanced neurophysiology in the prognostic and diagnostic evaluation of disorders of consciousness: review of an IFCN-endorsed expert group. *Clin Neurophysiol* 2020;**131**:2736–65.

Comolatti R, Pigorini A, Casarotto S *et al.* A fast and general method to empirically estimate the complexity of brain responses to transcranial and intracranial stimulations. *Brain Stimul* 2019;**12**:1280–9.

Compte A, Sanchez-Vives MV, McCormick DA *et al.* Cellular and network mechanisms of slow oscillatory activity (<1 Hz) and wave propagations in a cortical network model. *J Neurophysiol* 2003;**89**:2707–25.

Dalley JW, Cardinal RN, Robbins TW. Prefrontal executive and cognitive functions in rodents: neural and neurochemical substrates. *Neurosci Biobehav Rev* 2004;**28**:771–84.

David O, Kilner JM, Friston KJ. Mechanisms of evoked and induced responses in MEG/EEG. *NeuroImage* 2006;**31**:1580–91.

Dehaene S. *Consciousness and the Brain: Deciphering How the Brain Codes Our Thoughts*. Reprint edn. Westminster, London, England: Penguin Publishing Group, 2014.

Dehaene S, Changeux J-P, Naccache L. The global neuronal workspace model of conscious access: from neuronal architectures to clinical applications. In: Dehaene S, Christen Y (eds), *Characterizing Consciousness: From Cognition to the Clinic?* Berlin, Heidelberg: Springer, 2011, 55–84.

Del Cul A, Dehaene S, Reyes P *et al.* Causal role of prefrontal cortex in the threshold for access to consciousness. *Brain* 2009;**132**:2531–40.

Demertzi A, Tagliazucchi E, Dehaene S *et al.* Human consciousness is supported by dynamic complex patterns of brain signal coordination. *Sci Adv* 2019;**5**:eaat7603.

Esser SK, Hill SL, Tononi G. Sleep homeostasis and cortical synchronization: I. Modeling the effects of synaptic strength on sleep slow waves. *Sleep* 2007;**30**:1617–30.

Ferenets R, Lipping T, Anier A *et al.* Comparison of entropy and complexity measures for the assessment of depth of sedation. *IEEE Trans Biomed Eng* 2006;**53**:1067–77.

Fernandez LMJ, Comte JC, Le Merre P *et al.* Highly dynamic spatiotemporal organization of low-frequency activities during behavioral states in the mouse cerebral cortex. *Cereb Cortex* 2017;**27**:5444–62.

Ferro M, Lamanna J, Ripamonti M *et al.* Functional mapping of brain synapses by the enriching activity-marker SynaptoZip. *Nat Commun* 2017;**8**:1229.

Funk CM, Peelman K, Bellesi M *et al.* Role of somatostatin-positive cortical interneurons in the generation of sleep slow waves. *J Neurosci* 2017;**37**:9132–48.

Gao R, Peterson EJ, Voytek B. Inferring synaptic excitation/inhibition balance from field potentials. *NeuroImage* 2017;**158**:70–8.

Gao S, Calderon DP. Robust alternative to the righting reflex to assess arousal in rodents. *Sci Rep* 2020;**10**:20280.

Ghoneim MM, Block RI, Haffarnan M *et al.* Awareness during anesthesia: risk factors, causes and sequelae: a review of reported cases in the literature. *Anesth Analg* 2009;**108**:527–35.

Giacino JT, Kalmar K, Whyte J. The JFK coma recovery scale-revised: measurement characteristics and diagnostic utility. *Arch Phys Med Rehabil* 2004;**85**:2020–9.

Helfrich RF, Fiebelkorn IC, Szczepanski SM *et al.* Neural mechanisms of sustained attention are rhythmic. *Neuron* 2018;**99**:854–65.e5.

Kapoor V, Dwarakanath A, Safavi S *et al.* Decoding the contents of consciousness from prefrontal ensembles. *BioRxiv* 2020. https://www.biorxiv.org/content/10.1101/2020.01.28.921841v1.abstract.

Koch C, Massimini M, Boly M, Tononi G. Neural correlates of consciousness: progress and problems. *Nat Rev Neurosci* 2016;**17**:307–21.

Lau H, Rosenthal D. Empirical support for higher-order theories of conscious awareness. *Trends Cogn Sci* 2011;**15**:365–73.

Laureys S, Celesia GG, Cohadon F *et al.* Unresponsive wakefulness syndrome: a new name for the vegetative state or apallic syndrome. *BMC Med* 2010;**8**:68.

Lendner JD, Helfrich RF, Mander BA *et al.* An electrophysiological marker of arousal level in humans. *eLife* 2020;**9**:e55092.

Levinson M, Podvalny E, Baete SH *et al.* Cortical and subcortical signatures of conscious object recognition. *Nat Commun* 2021;**12**:2930.

Li D, Mashour GA. Cortical dynamics during psychedelic and anesthetized states induced by ketamine. *NeuroImage* 2019;**196**:32–40.

Linassi F, Zanatta P, Tellaroli P *et al.* Isolated forearm technique: a meta-analysis of connected consciousness during different general anaesthesia regimens. *Br J Anaesth* 2018;**121**:198–209.

Lombardi F, Herrmann HJ, de Arcangelis L. Balance of excitation and inhibition determines 1/f power spectrum in neuronal networks. *Chaos* 2017;**27**:047402.

Loomis AL, Harvey EN, Hobart GA. Cerebral states during sleep, as studied by human brain potentials. *J Exp Psychol* 1937;**21**:127.

Luppi AI, Craig MM, Pappas I *et al.* Consciousness-specific dynamic interactions of brain integration and functional diversity. *Nat Commun* 2019;**10**:4616.

Luppi AI, Golkowski D, Ranft A *et al.* Brain network integration dynamics are associated with loss and recovery of consciousness induced by sevoflurane. *Hum Brain Mapp* 2021;**42**:2802–22.

Maksimow A, Särkelä M, Långsjö JW *et al.* Increase in high frequency EEG activity explains the poor performance of EEG spectral entropy monitor during S-ketamine anesthesia. *Clin Neurophysiol* 2006;**117**:1660–8.

Mashour GA, Roelfsema P, Changeux JP, Dehaene S. Conscious processing and the global neuronal workspace hypothesis. *Neuron* 2020;**105**:776–98.

Massimini M, Huber R, Ferrarelli F *et al.* The sleep slow oscillation as a traveling wave. *J Neurosci* 2004;**24**:6862–70.

Massimini M, Huber R, Ferrarelli F *et al.* A perturbational approach for evaluating the brain's capacity for consciousness. *Prog Brain Res* 2009;**177**:201–14.

Mukovski M, Chauvette S, Timofeev I *et al.* Detection of active and silent states in neocortical neurons from the field potential signal during slow-wave sleep. *Cereb Cortex* 2007;**17**:400–14.

Murphy M, Huber R, Esser S *et al.* The cortical topography of local sleep. *Curr Top Med Chem* 2011;**11**:2438–46.

Nielsen TA. A review of mentation in REM and deep stages of sleep: "covert" REM sleep as a possible reconciliation of two opposing models. *Behav Brain Sci* 2000;**23**:851–66. discussion 904–1121.

Noreika V, Jylhänkangas L, Móró L *et al.* Consciousness lost and found: subjective experiences in an unresponsive state. *Brain Cogn* 2011;**77**:327–34.

Odegaard B, Knight RT, Lau H. Should a few null findings falsify prefrontal theories of conscious perception? *J Neurosci* 2017;**37**:9593–602.

Owen AM, Coleman MR, Boly M *et al.* Detecting awareness in the vegetative state. *Science* 2006;**313**:1402.

Pal D, Dean JG, Liu T *et al.* Differential role of prefrontal and parietal cortices in controlling level of consciousness. *Curr Biol* 2018;**28**:2145–52.e5.

Pal D, Li D, Dean JG *et al.* Level of consciousness is dissociable from electroencephalographic measures of cortical connectivity, slow oscillations, and complexity. *J Neurosci* 2020;**40**:605–18.

Paxinos G, Watson C. *The Rat Brain in Stereotaxic Coordinates*. 6th edn. Cambridge, MA: Academic Press, 2007.

Pigorini A, Sarasso S, Proserpio P *et al.* Bistability breaks-off deterministic responses to intracortical stimulation during non-REM sleep. *NeuroImage* 2015;**112**:105–13.

Poulet JFA, Crochet S. The cortical states of wakefulness. *Front Syst Neurosci* 2018;**12**:64.

Rosanova M, Fecchio M, Casarotto S *et al.* Sleep-like cortical OFF-periods disrupt causality and complexity in the brain of unresponsive wakefulness syndrome patients. *Nat Commun* 2018;**9**:4427.

Sanders RD, Tononi G, Laureys S *et al.* Unresponsiveness ≠ unconsciousness. *Anesthesiology* 2012;**116**:946–59.

Sarasso S, Casali AG, Casarotto S *et al.* Consciousness and complexity: a consilience of evidence. *Neurosci Conscious* 2021.

Sarasso S, Boly M, Napolitani M *et al.* Consciousness and complexity during unresponsiveness induced by propofol, xenon, and ketamine. *Curr Biol* 2015;**25**:3099–105.

Schartner MM, Seth A, Noirhomme Q *et al.* Complexity of multidimensional spontaneous EEG decreases during propofol induced general anaesthesia. *PLoS One* 2015;**10**:e0133532.

Seamans J. Losing inhibition with ketamine. *Nat Chem Biol* 2008;**4**:91–3.

Siclari F, Baird B, Perogamvros L *et al.* The neural correlates of dreaming. *Nat Neurosci* 2017;**20**:872–8.

Siclari F, Bernardi G, Cataldi J *et al.* Dreaming in deep stages of sleep: a high-density EEG study of slow waves and spindles. *J Neurosci* 2018;**38**:9175–85.

Siegle JH, López AC, Patel YA *et al.* Open Ephys: an open-source, plugin-based platform for multichannel electrophysiology. *J Neural Eng* 2017;**14**:045003.

Solms M. Dreaming and REM sleep are controlled by different brain mechanisms. *Behav Brain Sci* 2000;**23**:843–50. discussion 904–1121.

Steriade M, Amzica F, Contreras D. Synchronization of fast (30-40 Hz) spontaneous cortical rhythms during brain activation. *J Neurosci* 1996;**16**:392–417.

Steriade M, Nuñez A, Amzica F. A novel slow (< 1 Hz) oscillation of neocortical neurons in vivo: depolarizing and hyperpolarizing components. *J Neurosci* 1993;**13**:3252–65.

Steriade M, Timofeev I, Grenier F. Natural waking and sleep states: a view from inside neocortical neurons. *J Neurophysiol* 2001;**85**:1969–85.

Tononi G. An information integration theory of consciousness. *BMC Neurosci* 2004;**5**:42.

Tononi G, Boly M, Massimini M *et al.* Integrated information theory: from consciousness to its physical substrate. *Nat Rev Neurosci* 2016;**17**:450–61.

Tononi G, Edelman GM. Consciousness and complexity. *Science* 1998;**282**:1846–51.

Tononi G, Massimini M. Why does consciousness fade in early sleep? *Ann N Y Acad Sci* 2008;**1129**:330–4.

Valomon A, Riedner BA, Jones SG *et al.* A high-density electroencephalography study reveals abnormal sleep homeostasis in patients with rapid eye movement sleep behavior disorder. *Sci Rep* 2021;**11**:4758.

van Vugt B, Dagnino B, Vartak D *et al.* The threshold for conscious report: signal loss and response bias in visual and frontal cortex. *Science* 2018;**360**:537–42.

Vanhaudenhuyse A, Charland-Verville V, Thibaut A *et al.* Conscious while being considered in an unresponsive wakefulness syndrome for 20 years. *Front Neurol* 2018;**9**:671.

Vesuna S, Kauvar IV, Richman E *et al.* Deep posteromedial cortical rhythm in dissociation. *Nature* 2020;**586**:87–94.

Volgushev M, Chauvette S, Mukovski M, Timofeev I. Precise long-range synchronization of activity and silence in neocortical neurons during slow-wave sleep. *J Neurosci* 2006;**26**:5665–72.

Vyazovskiy VV, Olcese U, Hanlon EC *et al.* Local sleep in awake rats. *Nature* 2011;**472**:443–7.

Vyazovskiy VV, Olcese U, Lazimy YM *et al.* Cortical firing and sleep homeostasis. *Neuron* 2009;**63**:865–78.

Weilnhammer V, Fritsch M, Chikermane M *et al.* An active role of inferior frontal cortex in conscious experience. *Curr Biol* 2021;**31**:2868–80.e8.

Zingg B, Hintiryan H, Gou L *et al.* Neural networks of the mouse neocortex. *Cell* 2014;**156**:1096–111.